

Roughness of equipotential lines due to a self-affine boundary

This article has been downloaded from IOPscience. Please scroll down to see the full text article.

2006 J. Phys.: Condens. Matter 18 3393

(<http://iopscience.iop.org/0953-8984/18/13/007>)

View [the table of contents for this issue](#), or go to the [journal homepage](#) for more

Download details:

IP Address: 129.252.86.83

The article was downloaded on 28/05/2010 at 09:17

Please note that [terms and conditions apply](#).

Roughness of equipotential lines due to a self-affine boundary

Thiago A de Assis, Fernando de B Mota, José G V Miranda,
Roberto F S Andrade, Hugo de O Dias Filho and Caio M C de Castilho¹

Instituto de Física, Universidade Federal da Bahia, Campus Universitário da Federação,
40210-340, Salvador, BA, Brazil

E-mail: caio@ufba.br

Received 18 January 2006, in final form 7 February 2006

Published 13 March 2006

Online at stacks.iop.org/JPhysCM/18/3393

Abstract

In this work, the characterization of the roughness of a set of equipotential lines ℓ , due to a rough surface held at a nonzero voltage bias, is investigated. The roughness of the equipotential lines reflects the roughness of the profile, and causes a rapid variation in the electric field close to the surface. An ideal situation was considered, where a well known self-affine profile mimics the surface, while the equipotential lines are numerically evaluated using Liebmann's method. The use of an exact scale invariant profile helps to understand the dependency of the line roughness exponent $\alpha(\ell)$ on both the value of the potential (or on the average distance to the profile) and the profile's length. Results clearly support previous indications that: (a) for a system of fixed size, higher values of α characterize less corrugated lines far away from the profile; (b) for a fixed value of the potential, α decreases with the length of the profile towards the value of the boundary. This suggests that, for a system of infinite size, all equipotential lines share the same value of α .

(Some figures in this article are in colour only in the electronic version)

1. Introduction

The influence of boundary irregularities on the bulk properties of a medium is an important issue to the understanding of a large number of situations in many areas of natural sciences. It is well known that, for solid materials, the boundary effects are restricted to a few layers of atoms. However, in field and fluid problems, this influence can be dominant in a large length scale: for example, in electrostatic problems, where the presence of irregularities in a conducting charged surface propagates into the electric equipotential surfaces close to it; in diffusion of reactants to and from the surface of a catalyst; in stream lines of a flow in the slow

¹ Author to whom any correspondence should be addressed.

velocity Stokes regime, and so on. Depending on the system under consideration, a corrugate profile affects the motion of charged particles in a varying electric field, and the flow of matter to and from the catalyst, as well as the velocity field of the flow. Therefore, the investigation of the geometrical properties of these fields is of relevance not only for the characterization of the medium itself, but also for obtaining a detailed description of the dynamics of objects in such region.

A quantitative investigation of how deep the effect of an interface boundary can be propagated into the medium can be carried out with the help of several concepts and methods conceived within the framework of fractal geometry. These concepts have proved to be of importance in many areas of natural sciences, including surface science. Of course, this investigation is preceded by the evaluation of the field in the region bounded by the irregular profiles.

In this work we resume previous investigations [1] and consider the influence of a conducting rough charged surface on the electric field intensity close to the profile. This problem is motivated basically by the analysis of the motion of particles responsible for image formation in both field ion and field emission microscopies (FIM and FEM, respectively). The importance of extra [2] and local magnification [3] as a result of curvature of evaporated species in the atom-probe is well known. Effects resulting from local field variations can be also of practical interest in other areas, for example for determining the properties of devices and emitters [4], variation of the local work function [5, 6] and behaviour of electrodes [7, 8].

In previous works, we have analysed this problem and developed methodologies that were applied to regions bounded by profiles $y_1(x)$, held at a constant potential strength $\phi_0 = 0$, represented by the Koch curve [9], by Weierstrass functions [1, 10] and also by random profiles obtained from well known deposition algorithms [11]. In all previously investigated cases, the second boundary has been chosen to be a straight line $y_2(x) = Y_2$ placed far away from the maximal value of the profile, and held at $\phi_{y_2} = \phi_2 = 100$. Eventually $\phi_2 \rightarrow \infty$ when $y_2 \rightarrow \infty$. In the present work, the boundary $y_1(x)$ is represented by a geometrically generated self-affine profile. Although this is a relatively simpler situation than those obtained by random profiles, this investigation takes advantage of the *exact* scale invariance to clear out two seemingly conflicting scaling behaviour of the equipotential lines suggested by previous investigations: (i) the fractal dimension $D_f = 2 - \alpha$, where α is the roughness exponent, decreases together with ϕ as the average distance from the equipotential line to $y_1(x)$ increases; (ii) for a fixed potential line, D_f increases with the length L of the profile, suggesting that, as L increases, all lines might be characterized by the same value of D_f .

The fractal properties of the equipotential profiles are computed in the region confined by the two conductors as already described. The solution of Laplace's equation is numerically obtained at the region of interest, while the roughness exponent α and the fractal dimension $D_f = 2 - \alpha$ of the equipotential lines are evaluated with the help of the semivariogram method.

2. Methodology

The exact geometrical invariant rough profile used herein (see figure 1) has been adopted by a large number of authors. It is generated starting, at generation G_1 , by straight line segments linking successively the points $(x, y) = (0, 0), (1, 1), (2, 0), (3, 1)$ and $(4, 2)$. A comparison of figures in two successive generations indicates that all horizontal lengths have been expanded by a scaling factor $s_h = 4$, while the vertical scaling factor is $s_v = 2$. The initial states of this exact self-affine construction have been illustrated in several texts on fractal geometry so that, in figure 1, we just show the final figure at the eighth generation. For the purpose of avoiding undesirable boundary effects, we use only half of the points in each generation so that, for G_8 ,

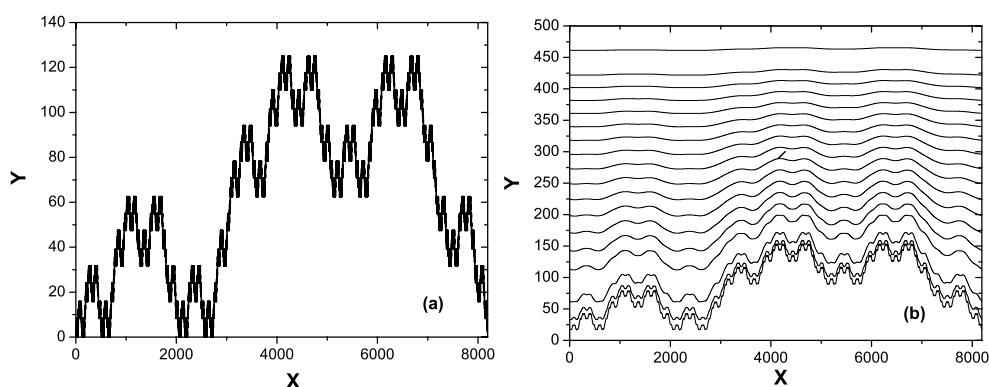


Figure 1. (a) Self-affine profile mimicking a rough boundary. (b) Equipotential lines $\phi(x) = \phi_i$, $\phi_i = 1, 7, 5n$, $n = 2, \dots, 20$, for the profile shown in (a). $\phi = 100$ at the upper boundary is an approximation of $\phi(y \rightarrow \infty) \rightarrow \infty$.

the profile has 8192 points. The roughness exponent $\alpha = \log(s_v)/\log(s_h)$ for this profile can be obtained exactly, the correct value $\alpha = 0.5$ being reproduced also by numerical procedures.

Laplace's equation

$$\Delta\phi = 0 \quad (1)$$

has been solved in the domain between the two conductors with the help of Liebmann's method [12]. The domain has been converted into a two-dimensional grid and the potential is iteratively calculated at each grid point for fixed and boundary conditions at $y_1(x)$ and $y_2(x)$, while periodic boundary conditions are imposed on the lateral borders.

Once the solution for (1) is available, a set of equipotential lines $y_{\phi_i}(x)$, $i = 1, \dots, M$ is obtained by performing linear extrapolations from the grid values of ϕ . The roughness properties of each profile, $y_{\phi_i}(x)$, follows its own scaling law, expressed by the roughness exponent α , which is measured with the help of the semivariogram algorithm [13]. It is based on the evaluation of the semivariance $\gamma(r)$, defined by

$$\gamma_{\phi_i}(r) = \frac{1}{2n(r)} \sum_{i=1}^{n(r)} [y_{\phi_i}(x) - y_{\phi_i}(x+r)]^2, \quad (2)$$

where, as already mentioned, $y_{\phi_i}(x)$ indicates the value of y for the potential value ϕ , at the value x , and $n(r)$ is the number of point pairs along the profile which are separated by a distance r . If we consider the roughness of the profile, which essentially measures how the largest height difference between any two points obeys a scaling law, it is possible to show that γ asymptotically depends on r as

$$\gamma_{\phi_i}(r) \sim r^{2\alpha_i}, \quad (3)$$

from which the value for α_i , corresponding to the equipotential ϕ_i , is computed.

3. Results and discussion

To better understand the results for the equipotential profiles, we have divided the discussion into two parts. First we present the results that arise when we work with a fixed number of points in the profile. In figure 1(b) we show, for $L = 8192$ points, a set of equipotential lines. The 19 lines shown were obtained, for this specific case, by holding $\phi_{y_1}(x) = 0$ and

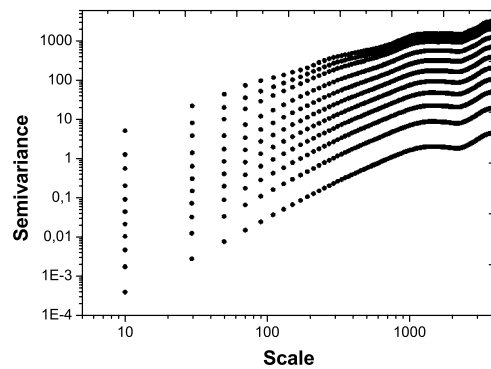


Figure 2. (a) Normalized semivariograms for an equipotential family for the Weierstrass profile. Lines far away from the profile have steeper slopes in the $r \rightarrow 0$ limit, corresponding to smaller values for D_f . Solid circles indicate, downward, equipotentials for $\phi = 1, 5$ and $10n$, $n = 1, 2, \dots, 9$.

$\phi_{y_2}(x) = 100$. However, the evaluation of the exponents α_i were performed for $i = 1, \dots, 100$. Note that, as $y_2 = 500$, the region where Laplace's equation was solved is highly asymmetrical, in the sense that the length of the profile is much larger than the maximal allowed value of y . This can, in principle, be justified by the following observations: by the geometrical construction, the maximal distance between the extremal sites in the x direction increases by a factor of 4 in each step of the construction of the profile, while in the y direction it increases only by a factor of 2. So, the maximal height of the profile increases with the length L as $L^{1/2}$. Then, the explicit solution of (1) shows that the shape of the equipotential lines close to the rough profile rapidly becomes insensitive to the boundary conditions. In such a situation they only slightly depend on the details of the numerical procedure, for example, on how far we have set the upper conductor. For instance, if we double the integration range of y and set $\phi(y = 1000) = 200$, this has little effect on the actual form of the equipotential lines for $\phi \approx 100$. Thus, in order to avoid unnecessary increase of CPU time and data storage, which adds almost no new significant information, we can indeed restrict the integration to the indicated region.

In figure 2 we illustrate some typical semivariograms in double logarithmic plots for several equipotential lines with $L = 8192$. Note that the largest scale roughly corresponds to $1/2$ of the whole profile, so that any point in γ represents an average value taken over a minimum of two distinct measurements. The log-log shape of all semivariograms $\gamma_{\phi_i}(r)$ consists, at small distances, of points aligned along a straight line with well defined slope. However, at large distances, the slope decreases and the $\gamma_{\phi_i}(r)$ have a tendency to saturate, building up a nearly horizontal plateau. This is related to fact that, since the profile is finite, its maximal height is also finite. The same effect is observed for all members of the family of equipotential lines.

As usual, the values of α have been obtained by a least square procedure, for a fixed range of values of $r/L \leq 0.4$. Of course this interval is bounded to the scaling region located prior to the saturation plateau. The results indicate larger values of α for larger values of ϕ . This increase in the value of α , to which is associated a decrease of the D_f , reflects the fact that the equipotential lines become less corrugated at larger distances to y_1 .

In order to better understand the dependence of D_f with respect to the electric potential and distance, in figure 3(a) we drew $D_f - 1$ as function of ϕ , while in figure 3(b) $D_f - 1$ is

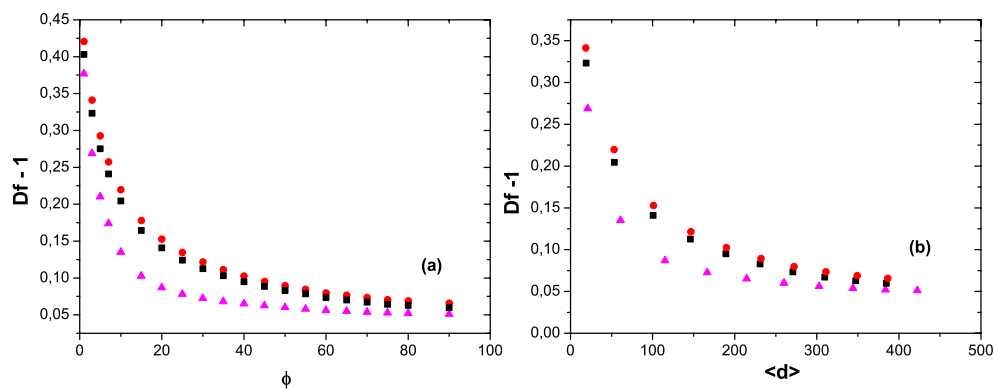


Figure 3. (a) Behaviour of $D_f - 1$ as a function of the potential ϕ for the three profiles. (b) Dependence of $D_f - 1$ as a function of the average distance $\langle d(\phi) \rangle$ with respect to ϕ . Solid circles, squares and triangles indicate, respectively, profiles with 8192, 4096 and 2048 points.

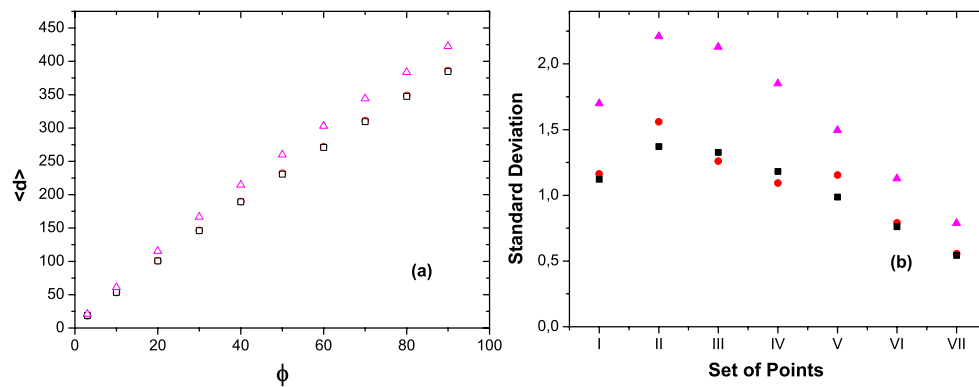


Figure 4. (a) Dependence of the average distance $\langle d(\phi) \rangle$ with respect to the potential. Hollow circles, squares and triangles indicate, respectively, profiles with 8192, 4096 and 2048 points. (b) Standard deviation for a linear fitting of sets of four successive points. Sets are formed such that set I corresponds to points 1, 2, 3 and 4, set II to points 2, 3, 4 and 5, and so on.

plotted as a function of $\langle d(\phi_i) \rangle$, which is defined as

$$\langle d(\phi) \rangle = \frac{1}{L} \sum_{x=0}^L [y_{\phi_i}(x) - y_{\phi=0}(x)]. \tag{4}$$

As expected, $\langle d(\phi_i) \rangle$ increases monotonically with ϕ , but no simple relation is obtained between the two quantities. Figure 4(a) suggests that there are two limit regions, for small and large values of ϕ , where the dependence is nearly linear but, for mid-range values, this simple dependence is lost. Indeed, an evaluation of the correlation coefficient and/or the standard deviation on groups of four consecutive points can corroborates this. For each set of ten points shown in figure 4(a), we have calculated the angular coefficient for the best straight line fitting four successive points. Thus, set I corresponds to the fitting of points 1, 2, 3 and 4, set II to points 2, 3, 4 and 5, and so on. Hence, set VII corresponds to the linear fitting of points 7, 8, 9 and 10. In figure 4(b), the standard deviation for the angular coefficients, for each set of four points, is shown. The results are poorer for mid-range values, as stated before, and indicate that, as d and $\phi \rightarrow \infty$, strict linearity is met.

Despite the general monotonic decay tendency of the set of points in figures 3(a) and (b), none of them can be accurately approximated by exponential or power laws. This same feature has been present in the results for the other random profiles [1] with the same exponent α . Since we are considering here a most regular rough profile, this result suggests an actual non-trivial dependence between D_f and ϕ or $\langle d(\phi_i) \rangle$.

As a second part of our results, we considered the dependence of the roughness properties of the equipotential lines, as a function of the length of the profile, L . This procedure is of great importance in understanding how a sequence of results for finite size samples can indicate what kind of behaviour is expected to be found in the limit of infinite size systems.

Since we wanted to follow the properties of equipotential lines upon increasing the size L of the system, it is important to establish a mapping between the lines $\phi_i(L_1)$ and $\phi_i(L_2)$ that will be brought into comparison. In principle, this task could be simply achieved by considering the value of ϕ by the average distance $\langle d(\phi) \rangle$. However, especially when we are close to the profile $y_1(x)$, there may be some small fluctuations arising from finite size effects of the periodic boundary conditions or from the value held fixed at y_2 , which replaces the actual boundary condition $\phi(y = \infty) = \infty$. In this work, we used the same procedure adopted before, which amounts to comparing equipotential lines with the same value of $\langle d(\phi) \rangle$.

To carry on the proposed comparison, we observed that it is not necessary to sequentially solve Laplace's equation for systems with increasing values of L . Indeed, we can restrict ourselves to integration of equation (1) just for the largest L_{\max} profile which we are able to handle, within the practical limits of the available computational facilities. Then it is sufficient to consider the same equipotential lines for patches L of different sizes $L_0 \leq L \leq L_{\max}$ and to evaluate the roughness exponent α for each one of them. On the one hand, the computational effort is greatly reduced and, besides that, it becomes possible to analyse patches sufficiently far away from the profile end points. In adopting this approach, not only can the influence of the boundary conditions on α be avoided, but also we get rid of the problem of performing the identification of equipotential lines stemming from distinct integration steps.

As the length L increases, the r interval where the scaling behaviour of $\gamma(r)$ is observed also increases, so that the values of α depend on the even larger lengths of the fitting interval. We have taken care to consider $r_{\max} = L/4$, so that, even for $L = L_{\max}$, we can obtain the value of α based on four distinct measures. For smaller values of L , results for α are actually based on a ever-growing number of distinct measurements.

4. Conclusions

In this work we have investigated the scaling properties of a family of equipotential lines for the Laplace problem in a region bounded by an exact scale invariant self-affine profile. The results we have obtained are in accordance to those of previous investigations, when deterministic or random profiles with only statistical scale invariance were considered. We have used herein two distinct ways regarding the results, confirming, in a much clearer way, two apparently contradictory results: the fractal dimension of equipotential lines of a profile with fixed length decreases when they get away from the profile, but increases with the increase of the profile. For an infinite profile, all lines should then share the same value of roughness exponent.

The correct interpretation of these results, however, is that it considers only the *scaling* properties of equipotential lines. In the limit of an infinite system, properties like the electric field and others that are derived from the potential depends on the distance to y_1 . Indeed, as the field is associated to the gradient of the potential, its intensity decays with the distance to y_1 , as exemplified by the generation of atomic images in a field ion microscope.

Acknowledgments

The authors acknowledge the financial support of CNPq, CAPES and FAPESB, Brazilian agencies. This work has partial support of FINEP-CTPETRO/FAPEX/UFBA (contract 65.99.0487.00). Mrs A C F de Castilho was very helpful in revising the text.

References

- [1] Dias Filho H de O, de Castilho C M C, Miranda J G V and Andrade R F S 2004 *Physica A* **342** 388
- [2] Brenner S S and McKinney J T 1970 *Surf. Sci.* **23** 88
- [3] Miller M K and Hetherington M G 1991 *Surf. Sci.* **246** 442
- [4] Woodruff P and Delchar T A 1994 *Modern Techniques of Surface Science* 2nd edn (Cambridge: Cambridge University Press)
- [5] Brodie I 1995 *Phys. Rev. B* **51** 13660
- [6] Wojciechowski K F 1997 *Europhys. Lett.* **38** 135
- [7] Filoche M and Sapoval B 2000 *Electrochim. Acta* **46** 213
- [8] de Levie R 1965 *Electrochim. Acta* **10** 113
- [9] Cajueiro D O, Sampaio V A de A, de Castilho C M C and Andrade R F S 1999 *J. Phys.: Condens. Matter* **11** 4985
- [10] Feder J 1988 *Fractals* (New York: Plenum)
- [11] Barabási A-L and Stanley H E 1995 *Fractal Concepts in Surface Growth* (Cambridge: Cambridge University Press)
- [12] Gerald C F and Wheatley P O 1985 *Applied Numerical Analysis* 3rd edn (New York: Addison-Wesley)
- [13] Russ J C 1994 *Fractal Surfaces* (New York: Plenum)